

Particle acceleration at shocks in relativistic jets

J.G. Kirk

Max-Planck-Institut für Kernphysik, Postfach 10 39 80, D-69029
Heidelberg, Germany

Abstract: The theory of particle acceleration at shock fronts is briefly reviewed, with special emphasis on the production of the particles responsible for the non-thermal emission from blazars. The flat radio/IR spectra of these sources cannot be produced by diffusive acceleration at a simple nonrelativistic shock front propagating in a homogeneous medium. It can, however, be produced by a single unmodified mildly relativistic shock, if the pressure in the shocked gas is provided by the leptonic component, or, independently of the equation of state, by a relativistic shock which is oblique to the magnetic field. The analytic theory of these shocks makes several simplifications, but Monte-Carlo simulations exist which extend the range of validity. Of particular interest is acceleration in a tangled magnetic field. Here, however, the Monte-Carlo simulations have not yet yielded unambiguous results. The ‘homogeneous’ models of blazar emission are discussed, and it is shown that they imply a geometry of the emitting region which is laminar in form, with an aspect ratio of $d/R \leq 3\%$ in the case of Mkn 421. Identifying these with relativistic shock fronts, a model of acceleration is described, which displays characteristic variations in the synchrotron spectral index with intensity.

1 Introduction

The problem of how particles are accelerated to nonthermal energies in relativistic jets has been discussed for a number of years (e.g., Begelman, Blandford & Rees 1984). Diffusive acceleration at nonrelativistic shocks is a possibility which appears to provide a reasonable picture of acceleration at several jet hot-spots which emit optical synchrotron radiation (Meisenheimer et al. 1989). However, the rapid variability of emission from blazar jets implies substantial doppler boosting, which suggests that the nonrelativistic theory may be inappropriate. Relativistic shocks have also been known for some time to be potentially effective accelerators (Kirk & Schneider 1987), but, unlike their nonrelativistic counterparts, they do not lead to

a unique spectral index which is independent of the details of the scattering process and the shock speed. Instead, a wide range of spectral slopes is possible.

The best developed model of blazar spectra is based on the picture of a shock front moving down a jet (Marscher & Gear 1985). Both the magnetic field and the particle distribution vary with position, and the observed radiation is a superposition of emission from different parts of the jet (Ghisellini, Maraschi & Treves 1985, Ballard et al. 1990, Hughes, Aller & Aller 1991, Maraschi, Ghisellini & Celotti 1992, Levinson & Blandford 1995, Marscher & Travis 1996). These models are generally called ‘inhomogeneous’. However, recent results concerning the rapid variability of blazar sources at all frequencies (Wagner & Witzel 1995) and the detection of their emission at energies of up to at least 10 TeV (Aharonian et al. 1997) have provided new restrictions on the possible acceleration mechanisms. Especially the observed simultaneous variations in X-rays and TeV gamma-rays indicate that a single population of particles in a relatively localised region is responsible. Consequently, ‘homogeneous’ models have been widely discussed (Dermer & Schlickeiser 1993, Macomb et al. 1995, 1996, Bloom & Marscher 1996, Ghisellini, Maraschi & Dondi 1996, Inoue & Takahara 1996, Stecker, de Jager & Salamon 1996, Comastri et al. 1997, Mastichiadis & Kirk 1997) and there is rough agreement on the parameters of the emission region.

Simultaneous variability of emission at widely differing wavelengths is more easily interpreted in terms of directly accelerated electrons than in the hadronic models (Mannheim 1993, Mannheim et al. 1996), in which the gamma-ray emission stems originally from ultra-relativistic protons, and only the optical and (in some sources) X-ray photons arise from directly accelerated electrons. Protons and electrons are accelerated in regions of different spatial extent on very different timescales, because the waves which provide the scattering centres have a wavelength comparable to the particle’s gyro radius, and the acceleration time of a particle is probably somewhat longer than its gyro period. Consequently, one would expect the radiation produced by relatively low energy (GeV to TeV) electrons to have different variability properties to that produced by protons of energy above 1 EeV. However, further information concerning the emission of these objects at energies above 20 TeV (Meyer & Westerkhoff 1996) may well provide the most reliable way distinguishing between the leptonic and hadronic models.

2 Basic properties of shock acceleration

It is well-known that particles which diffuse in the neighbourhood of a non-relativistic shock front can be accelerated into a power-law distribution such that the density of particles with Lorentz factor γ is a power-law, $n(\gamma) \propto \gamma^{-s+2}$, with

$$s = 3\rho_c/(\rho_c - 1) \quad (1)$$

where ρ_c is the compression ratio of the shock front. The physical basis of acceleration is that an energetic particle scatters elastically off magnetic fluctuations in the background plasma, which enables it to cross and recross the shock front. Simple kinematics lead to an energy gain on each crossing, since, at a shock front, the scattering centres take part in the plasma compression. This competes with the possibility that a particle moves off into the downstream plasma and does not return, to yield a power-law spectrum (for a review see Kirk, Melrose & Priest 1994).

Before they have had time to cool, the synchrotron emission of electrons accelerated into a distribution described by Eq. (1) is a power law $I(\nu) \propto \nu^{-\alpha}$, with $\alpha = (s - 3)/2$. Thus, a strong nonrelativistic shock front in a fully ionised gas, which has $\rho_c = 4$, produces $\alpha = 0.5$. There are several effects which modify this result. However, most of them lead to a softening of the predicted spectrum, at least for lower energy electrons (e.g. Bell 1987, Ellison & Reynolds 1991, Duffy, Ball & Kirk 1995). In the case of blazars, the homogeneous model requires a harder spectrum – for Mrk 421, for example, $\alpha \approx 0.35$.

Blazar jets are almost certainly in relativistic motion, but although relativistic shocks offer a range of indices, the required $s = 3.7$ is not easily obtained. As shown in Fig. 1, mildly relativistic shocks ($0.1 < u_1 < 0.9$, with u_1 the speed of the shock seen from the rest frame of the upstream plasma) give this value provided the electron pressure is important behind the shock front. This effect is due not to a radical change in the way in which acceleration operates, but simply to the increased compression ratio across the shock front when electrons are heated to a temperature comparable with their rest-mass. Whether the processes mediating a relativistic shock lead to such heating is unknown. However, it seems unlikely that the background plasma, which is assumed to carry more energy flux than the accelerated component, should remain invisible, despite having an electron temperature of several MeV. A more attractive alternative is presented by oblique relativistic shocks. In contrast to the nonrelativistic case, where the obliquity has no effect on the spectral index (Axford 1980), oblique relativistic shocks show much harder spectra (Kirk & Heavens 1989), ranging up to $s = 3$. The reason for this behaviour lies in the increased importance of reflections from the shock front as a fundamental accelerating process. If particles are tightly bound to field lines, and are also randomly distributed in gyro-phase – two assumptions behind the analytic treatment of Kirk &

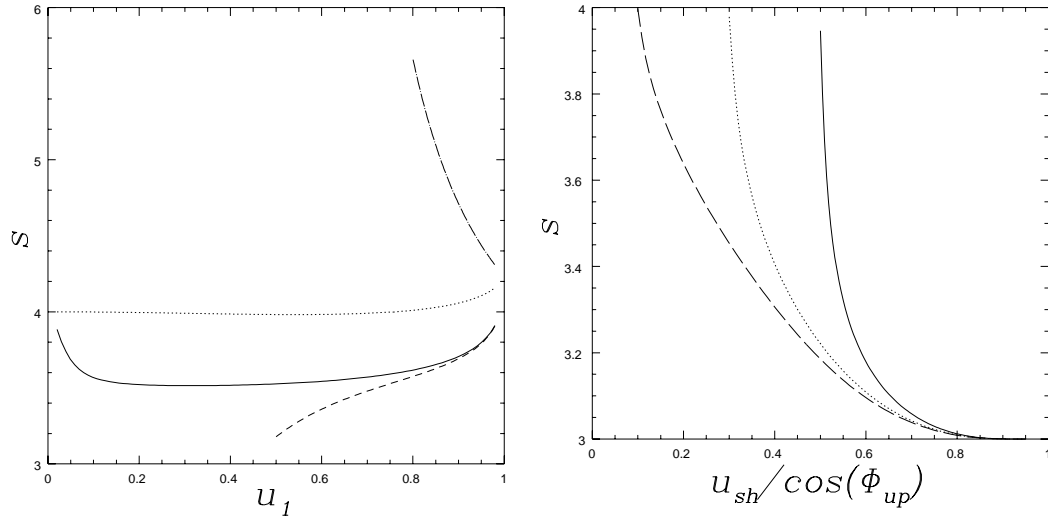


Fig. 1. The power law index of particles accelerated at a relativistic shock front. The left-hand panel shows the index s of the phase space-density for a parallel shock as a function of the velocity of the shock seen from the rest frame of the upstream plasma. Four different equations of state are used: the dashed-dotted line is for a relativistic gas, the dotted line for a gas in which the ions provide the pressure (i.e., hot ions, cold electrons), the solid line is for hot electrons and cold ions, and the dashed line is for a gas containing a population of electron positron pairs. A relatively hard spectrum is obtained for intermediate speeds if the electrons are hot, or pairs present. At high speeds ($\Gamma > 5$) all curves tend towards the value $s = 4.2$. In the right-hand panel, the effect of a finite angle Φ_{up} between the shock normal and the magnetic field is shown, for three different values of the upstream shock speed $u_{sh} = 0.1, 0.3$ and 0.5 and a compression ratio of 4. As the speed of the intersection point of the shock and field line ($= u_{sh} / \cos(\Phi_{up})$) approaches c , the spectra harden.

Heavens (1989) – the probability that they are reflected by the magnetic compression at the shock front is significant. As the shock speed increases, the energy gained on reflection goes up, since the effective speed of the ‘mirror’ is that of the intersection point of a magnetic field line with the shock surface. The overall effect is to harden the spectra as shown in Fig. 1.

It has been pointed out that this type acceleration might be suppressed in highly relativistic flows (Begelman & Kirk 1990). In the absence of cross-field transport, crossing and recrossing requires that a particle move faster along a field line than the intersection point of that line with the shock front. This speed will normally exceed c for a highly relativistic shock, unless the upstream field is aligned to within an angle of $1/\Gamma$ of the shock normal. (Here $\Gamma = (1 - u_1^2/c^2)^{-1/2}$ is the Lorentz factor associated with the speed

of the shock seen from the rest frame of the upstream plasma.) As a result, recrossing of the shock into the upstream medium would not be permitted and acceleration would be limited to a single encounter – a process usually referred to as ‘shock-drift’ acceleration.

The two main assumptions used in the analytic theory of relativistic oblique shocks (conservation of magnetic moment, and absence of cross-field transport) are readily relaxed in a Monte-Carlo simulation, and this program has been carried out by several groups (Ostrowski 1991, Lieu et al. 1994, Naito & Takahara 1995). The simulations show that the degree of cross-field transport is critical. The analytic results are reproduced if it is small, but the spectra soften to reach the value for a parallel shock once the transport properties become isotropic. Another feature emphasised by these simulations is that the spectrum produced depends upon the type of scattering used in the simulation – a property also of parallel relativistic shocks (Kirk & Schneider 1988).

Scattering is ultimately just one way of describing the perturbed trajectory of a particle which encounters fluctuations of the magnetic field about its average value. If, as would appear from the above work, the obliquity of the shock front is crucial, fluctuations might have an important role in changing the angle with which a particular field line hits the shock front, a process which is not included in simulations which simply superpose stochastic scattering on motion in a homogeneous field. To investigate this effect, two groups have performed simulations in which a tangled magnetic field with a random component is realised explicitly (Ballard & Heavens 1992, Ostrowski 1993). Assuming that the field is frozen into the plasma, which supports a shock front consisting of a simple velocity discontinuity, the particle orbits are followed by numerically integrating the equations of motion. From the considerations mentioned above, we might expect that reflection from the shock front plays the dominant role in such a situation. In fact, a tangled field will always inhibit the escape of a particle reflected off the advancing edge of the shock front and cause it to be caught once again. Thus, a layer of energised particles may well be built up on the upstream side of the shock front. On transmission to the downstream plasma, tangling of the field will in principle permit some particles to return to the shock front. In a highly oblique shock, this process is unimportant, which may also be the case at a relativistic shock with tangled fields. However, this is mere speculation; the two Monte-Carlo simulations unfortunately yield conflicting results, for reasons which have not yet been resolved. A possible explanation is that the techniques by which the stochastic field is realised are different in each simulation, and it is not clear that the statistical properties of the resulting field lines are equivalent.

Stochastic magnetic fields have recently been investigated in connection with cosmic ray transport (Chuvilgin & Ptuskin 1993) and with nonrelativistic shocks (Duffy et al. 1995, Kirk, Duffy & Gallant 1996), where they

have been shown to be one of the few effects capable of modifying the rather robust result given by Eq. (1). Simulation techniques which exploit this approach (Gieseler et al. 1997) may prove useful in resolving the question for relativistic shocks.

3 A model of the time dependence of acceleration

In the case of the homogeneous synchro-self-compton model, the following simple estimate can be made (cf. Takahashi et al. 1996). Denote by ν_{10} the highest energy photons emitted as synchrotron radiation in units of 10 keV, and by t_3 the variability timescale of this emission in thousands of seconds, which we identify with the cooling time by synchrotron radiation. Then $\nu_{10} \approx 10^{-12} \gamma^2 B \delta$ and $t_3 \approx 10^6 \gamma^{-1} B^{-2} \delta^{-1}$, where γ is the Lorentz factor of the particle in the rest frame of the emitting plasma, B the magnetic field in gauss and δ the Doppler boosting factor. These relations imply $B = 1 \times t_3^{-2/3} \nu_{10}^{-1/3} \delta^{-1/3}$ gauss and $\gamma = 10^6 \times t_3^{1/3} \nu_{10}^{2/3} \delta^{-1/3}$. Those objects which show TeV emission generally have roughly the same luminosity in the synchrotron and the inverse compton parts of the spectrum, which means that the energy densities of photons and magnetic field in the source are of comparable magnitude. Setting them equal leads to an expression for the ‘aspect ratio’ of the source region $\eta = d/R$, where $d = 1000 t_3 \delta / c$ is a characteristic thickness measured in the rest frame of the source, and R is defined such that πR^2 is the area of the source when projected onto the plane of the sky. For Mkn 421, which has an apparent luminosity of 6×10^{44} erg s $^{-1}$, one finds $\eta = 7 \times 10^{-5} \nu_{10}^{-1/3} t_3^{1/3} \delta^{8/3}$, and, inserting $\delta = 10$, $\nu_{10} = 1$ and $t_3 = 1$, we find $\eta \approx 0.03$. This indicates that we are dealing with an essentially two-dimensional source region, which it is tempting to identify with a relativistic shock front.

The observation of electrons during their acceleration by the shock front of SN1987A (Staveley-Smith et al. 1992) led to the development of a simple but useful model for the time-dependence of shock acceleration (Ball & Kirk 1992) which can be applied to the present case simply by generalising the kinematics to relativistic flows, and including the effects of synchrotron energy losses. The basic idea is to divide the system up into two regions: one – which we can imagine to be around or just in front of the shock front – in which particles are either repeatedly reflected, or cross and recross the front and so undergo continuous acceleration at a rate t_{acc}^{-1} , and a second which is the downstream plasma, where there is no further acceleration, but only cooling. Escape from the acceleration zone into the downstream plasma occurs at a rate t_{esc}^{-1} . The number $N(\gamma)d\gamma$ of particles in the acceleration zone with Lorentz factor between γ and $\gamma + d\gamma$ is governed by the equation

$$\frac{\partial N}{\partial t} + \frac{\partial}{\partial \gamma} \left[\left(\frac{\gamma}{t_{\text{acc}}} - \beta_s \gamma^2 \right) N \right] + \frac{N}{t_{\text{esc}}} = Q \delta(\gamma - \gamma_0) \quad (2)$$

(e.g., Kirk, Melrose & Priest 1994), where $\beta_s = 4\sigma_T/(3m_e c)(B^2/8\pi)$ with $\sigma_T = 6.65 \cdot 10^{-25} \text{cm}^2$ the Thomson cross section. The first term in brackets in Eq. (2) describes acceleration, the second describes the rate of energy loss due to synchrotron radiation averaged over pitch-angle in a magnetic field B (in gauss). Particles are assumed to be picked up (injected) into the acceleration process with Lorentz factor γ_0 at a rate Q particles per second.

In a one-dimensional picture, with the x coordinate along the shock normal the kinetic equation governing the differential density $dn(x, \gamma, t)$ of particles which have escaped into the downstream plasma and are in the range dx , $d\gamma$ is

$$\frac{\partial n}{\partial t} - \frac{\partial}{\partial \gamma}(\beta_s \gamma^2 n) = \frac{N(\gamma, t)}{t_{\text{esc}}} \delta(x - x_s(t)) \quad (3)$$

where $x_s(t)$ is the position of the shock front at time t , and a coordinate system has been used in which the plasma is at rest. Note that the ‘injection’ term in this equation is provided by those particles escaping the acceleration zone.

Equations (2) and (3) are simple to solve. Using the synchrotron Green’s function the electron distribution is then readily linked to the emitted radiation, given the time dependence of the rate Q at which particles are picked up by the acceleration process (Kirk, Rieger & Mastichiadis 1997). For example, a simple representation of a flare is found by setting $Q(t) = Q_0$ for $t < 0$ and $t > 10t_{\text{acc}}$ and $Q(t) = 2Q_0$ for $0 < t < 10t_{\text{acc}}$.

The corresponding synchrotron emission in the rest frame of the source is shown in Fig. 2. The behaviour of the spectrum at frequencies well below the maximum, where the acceleration time t_{acc} is much shorter than the synchrotron cooling time $(\beta_s \gamma)^{-1}$ shows the characteristic ‘slow-lag’ observed in several sources (e.g., Pks 2155–3034: Sembay et al. 1993 and Mkn 421: Takahashi et al 1996). This can be interpreted simply in terms of synchrotron cooling (Tashiro et al. 1995). However, closer to the maximum frequency, the finite acceleration time comes into play (At $\gamma = \gamma_{\text{max}}$, we have $t_{\text{acc}} = (\beta_s \gamma_{\text{max}})^{-1}$.) Then it is possible to produce hysteresis curves which are followed in the opposite direction, namely anti-clockwise. This behaviour is characteristic of the acceleration mechanism. Although the details of such loops will depend on factors neglected here such as the energy dependence of t_{acc} , inhomogeneities in the source geometry, and smoothing effects produced by the finite light travel time across the face of the source, the conclusion remains that anti-clockwise motion is the signature of the acceleration mechanism. Combined with the fact that rapid variation implies laminar source geometry and that substantial doppler boosting is required, this may also be the signature of a relativistic shock front.

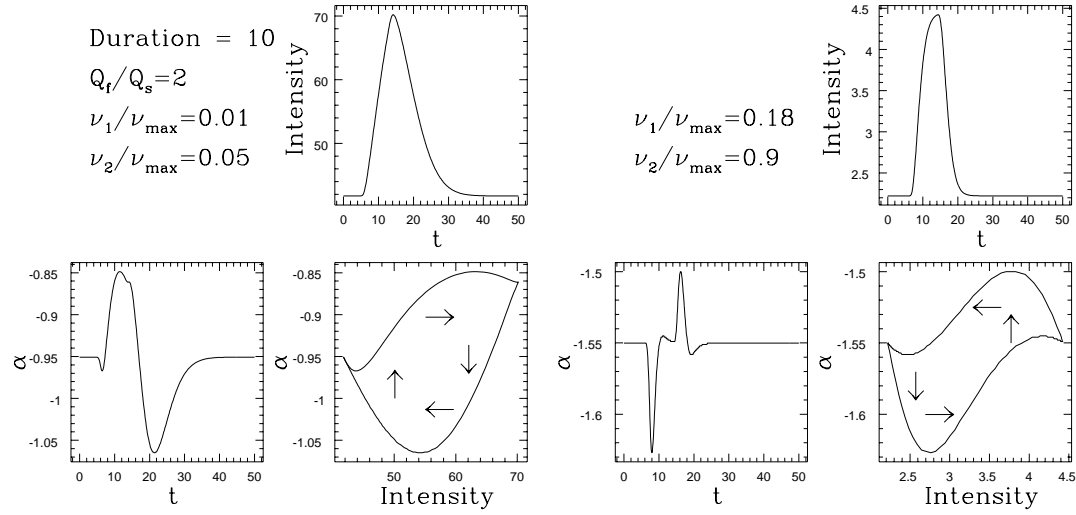


Fig. 2. The predicted behaviour of the synchrotron emission and spectral index during a flare. In the left-hand set of three panels, the light curve, and spectral index at low frequency ($\nu = \nu_{\max}/20$) are shown (with the index α calculated from the flux ratio at ν and $\nu/10$). The loop in the α vs. intensity plane is traversed in the clockwise direction. In the right-hand panels, the same plots are shown at $\nu = 0.9\nu_{\max}$. Here the loop is followed in the anti-clockwise direction.

References

- Aharonian F. et al. 1997 submitted to A&A
 Axford W.I. 1980 Proc. 17th. Int. Cosmic Ray Conf. (Paris) 12, 155
 Ball L., Kirk J.G. 1992 ApJ 396, L39
 Ballard K.R., Mead A.R.G., Brand P.W.J.L., Hough J.H. 1990 MNRAS 243, 640
 Ballard K.R., Heavens A.F. 1992 MNRAS 259, 89
 Begelman, M.C., Blandford R.D., Rees M.J. 1984 Reviews of Modern Physics 56, 255
 Begelman M.C., Kirk J.G. 1990 ApJ 353, 66
 Bell A.R. 1987 MNRAS 225, 615
 Bloom S.D., Marscher A.P. 1996 ApJ 461, 657
 Chuvilgin L.G., Ptuskin V.S. 1993 A&A 279, 278
 Comastri A., Fossati G., Ghisellini G., Molendi S. 1997 ApJ 480, 534
 Dermer C.D., Schlickeiser R. 1993 ApJ 416, 458
 Duffy P., Ball L., Kirk J.G. 1995 ApJ 447, 364
 Duffy P., Kirk J.G., Gallant Y.A., Dendy R.O. 1995 A&A 302, L21
 Ellison D.C., Reynolds S.P. 1991 ApJ 382, 242
 Ghisellini G., Maraschi L., Dondi L. 1996 A&A Supplement 120C, 503
 Ghisellini, G., Maraschi, L., Treves, A. 1985, A&A 146, 204

- Gieseler U.D.J., Duffy P., Kirk J.G., Gallant Y.A. 1997 Proc. 25th. Int. Cosmic Ray Conf. (Durban)
- Hughes P.A., Aller H.D., Aller M.F. 1991 ApJ 374, 57
- Inoue S., Takahara F. 1996 ApJ 463, 555
- Kirk J.G., Duffy P., Gallant Y.A. 1996 ApJ 314, 1010
- Kirk J.G., Heavens A.F. 1989 MNRAS 239, 995
- Kirk J.G., Rieger F.M., Mastichiadis A. 1997 in preparation
- Kirk J.G., Melrose D.B., Priest E.R. 1994 'Plasma Astrophysics' Springer-Verlag, New York
- Kirk J.G., Schneider P. 1987 ApJ 315, 425
- Kirk J.G., Schneider P. 1988 A&A 201, 177
- Lieu R., Quenby J.J., Drolas B., Naidu K. 1994 ApJ 421, 211
- Levinson A., Blandford R.D. 1995 ApJ 449, 86
- Macomb, D.J. et al. 1995 ApJ 449, L99
- Macomb, D.J. et al. 1996 ApJ 459, L111 (Erratum)
- Mannheim K. 1993 A&A 269, 67
- Mannheim K., Westerhoff S., Meyer H., Fink H.-H. 1996 A&A 315, 77
- Maraschi F., Ghisellini G., Celotti A. 1992 ApJ 379, L5
- Marscher A.P., Gear W.K. 1985 ApJ 298, 114
- Marscher A.P., Travis J.P. 1996 A&A Supplement 120C, 537
- Mastichiadis A., Kirk J.G. 1997 A&A 320, 19
- Meisenheimer K., Röser H.-J., Hiltner P.R., Yates M.G., Longair M.S., Chini R., Perley R.A. 1989 A&A 219, 63
- Meyer H., Westerhoff S. 1996 in 'Proceedings of the Heidelberg Workshop on Gamma-ray emitting AGN', Eds. J.G. Kirk, M. Camenzind, C. von Montigny, S. Wagner, MPI-Kernphysik internal report No. MPI H-V37-1996, page 39
- Naito T., Takahara F. 1995 MNRAS 275, 1077
- Ostrowski M. 1991 MNRAS 249, 551
- Ostrowski M. 1993 MNRAS 264, 248
- Sembay S., Warwick R.S., Urry C.M., Sokoloski J., George I.M., Makino F., Ohashi T., Tashiro M. 1993 ApJ 404, 112
- Staveley-Smith L. et al. 1992 Nature 355, 147
- Stecker F.W., de Jager O.C., Salamon M.H. 1996 ApJ 473, L75
- Takahashi, Tashiro, Madejski G., Kubo H., Kamae T., Kataoka J., Kii T., Makino F., Makishima K., Yamasaki N. 1996 ApJ 470, L89
- Tashiro et al. 1995 PASJ, 47, 131
- Wagner S.J., Witzel A. 1995 ARA&A 33, 163